(10) Hadjichristidis, N. *Makromol. Chem.* **1977**, *178*, 1463.
(11) Mays, J. W.; Ferry, W.; Hadjichristidis, N.; Fetters, L. J. *Macromolecules* **1985**, *18*, 2330.
(12) Yamakawa, H. *Modern Theory of Polymer Solutions*; Harper and Row: New York, 1971; Chapter 7.
(13) Shultz, A. R.; Flory, P. J. *J. Am. Chem. Soc.* **1952**, *74*, 4760.
(14) Berry, G.; Casassa, E. F. *J. Polym. Sci., Part D* **1970**, *4*, 1.
(15) Burchard, W. *Makromol. Chem.* **1961**, *50*, 20.
(16) Stockmayer, W. H.; Fixman, M. *J. Polym. Sci.* **1963**, *1*, 137.
(17) Stockmayer, W. H. *Br. Polym. J.* **1977**, *9*, 89.
(18) Flory, P. J. *J. Chem. Phys.* **1949**, *10*, 51.
(19) McIntyre, D.; Wims, A.; Williams, L. C.; Mandelkern, L. *J. Phys. Chem.* **1966**, *66*, 1932.
(20) Berry, G. C. *J. Chem. Phys.* **1967**, *46*, 4886.
(21) Fukuda, M.; Fukutomi, M.; Kato, Y.; Hashimoto, T. *J. Polym. Sci., Polym. Phys. Ed.* **1978**, *16*, 105.
(22) Norisuye, T.; Kawahara, K.; Teramoto, A.; Fujita, H. *J. Chem. Phys.* **1968**, *49*, 4330.
(23) Yamamoto, A.; Fujii, M.; Tanaka, G.; Yamakawa, H. *Polym. J. (Tokyo)* **1971**, *2*, 799.
(24) Miyake, Y.; Einaga, Y.; Fukita, M.; Fukada, M. *Macromolecules* **1980**, *13*, 588.
(25) Hadjichristidis, N.; Xu, Z.; Fetters, L. J.; Roovers, J. *J. Polym. Sci., Polym. Phys. Ed.* **1982**, *20*, 743.
(26) Sundararajan, P. R.; Flory, P. J. *J. Am. Chem. Soc.* **1974**, *96*, 5025.
(27) Sundararajan, P. R. *J. Polym. Sci., Polym. Lett. Ed.* **1977**, *15*, 699.
(28) Vacatello, M.; Flory, P. J. *Macromolecules* **1986**, *19*, 405.
(29) Sundararajan, P. R. *Macromolecules* **1986**, *19*, 415.
(30) Development of RIS models for polymers with complex side groups has been hindered because of the complifications inherent in taking into account the effects of various substituent conformations on polymer chain statistics.
(31) Bareiss, R. E. *Polymer Handbook*, 2nd ed.; Brandrup, J., Immergut, E. H., Eds.; Interscience: New York, 1975; pp iv–115.
(32) Brandrup, J., Immergut, E. H., Eds. *Polymer Handbook*, 2nd ed.; Interscience: New York, 1975; Part IV.
(33) Hadjichristidis, N.; Touloupis, C.; Fetters, L. J. *Macromolecules* **1981**, *14*, 128.
(34) Mays, J. W.; Hadjichristidis, N. *J. Macromol. Sci., Rev. Macromol. Chem. Phys.* **1988**, *C28(3&4)*, 371.
(35) Bohdanecky, M.; Kovar, J. *Viscosity of Polymer Solutions*; Elsevier: Amsterdam, 1982.
(36) De Gennes, P.-G. *Scaling Concepts in Polymer Physics*; Cornell University: Ithaca, NY, 1979.

Synthesis and Characterization of Liquid Crystalline Polymethacrylates, Polyacrylates, and Polysiloxanes Containing 4-Hydroxy-4′-methoxy-α-methylstilbene Based Mesogenic Groups

Virgil Percec* and Dimitris Tomazos

Department of Macromolecular Science, Case Western Reserve University, Cleveland, Ohio 44106-2699. *Received August 8, 1988*

ABSTRACT: The synthesis and characterization of polymethacrylates and polyacrylates containing 4-hydroxy-4′-methoxy-α-methylstilbene side groups attached through flexible spacers containing 11, 8, 6, 3, and 2 methylenic units and of the polysiloxanes containing the same mesogenic group connected through flexible spacers containing 11, 8, 6, and 3 methylenic units, respectively, are described. All polymers exhibit thermotropic liquid crystallinity. The nature of the mesophase is determined by the spacer length. However, the nature of the polymer backbone determines the thermal stability of the mesophase and the ease of the side-chain crystallization. That is, for the same spacer length and similar polymer molecular weight, the most flexible polymer backbone leads to the highest isotropization temperature and the highest ease of side-chain crystallization. This last effect may lead to transformation of enantiotropic mesophases into monotropic mesophases.

Introduction

Previous publications from our laboratory have suggested that side-chain liquid crystalline "copolymers" of monomer pairs containing constitutional isomeric mesogenic units are useful both to depress side-chain crystallization of polymers containing long flexible spacers and to obtain qualitative information about the degree of decoupling.[1-4] This idea was based on the fact that mesomorphic phases of the same type are usually miscible, while crystallization of two isomers is a more difficult process. Consequently, for a single-phase side-chain liquid crystalline copolymer based on constitutional isomeric side groups, we would expect side-chain crystallization to be depressed. Alternatively, for a microphase-separated side-chain liquid crystal polymer,[5-7] we would expect to observe independent crystallization of each isomer in part.[3]

Therefore, copolymers of constitutional isomeric groups may represent a chemical sensor which provides at least qualitative information on the dynamics of side-chain liquid crystalline polymers. If this assumption is correct, these copolymers can offer a qualitative and complimentary approach to the study of the dynamics of side-chain liquid crystalline polymers.[8-13]

The experiments performed so far were done with side groups based on 4-methoxy-4′-hydroxy-α-methylstilbene and 4-hydroxy-4′-methoxy-α-methylstilbene constitutional isomers. However, all monomer mixtures were prepared directly as mixtures of constitutional isomers, since they were synthesized by the monomethylation of 4,4′-dihydroxy-α-methylstilbene.[1-3] Although the molar ratio between the two constitutional isomeric side groups was determined by spectropical methods, no information about the behavior of each of the two homopolymers based on each individual constitutional isomer was available. In order to obtain a quantitative interpretation of these copolymers' behavior, the synthesis and characterization of the homopolymers based on each of the two constitutional isomers are mandatory. The synthesis and characterization of the polymethacrylates, polyacrylates, and polysiloxanes containing mesogenic groups based on 4-methoxy-4′-hydroxy-α-methylstilbene and flexible spacers containing 11, 8, 6, 3, and 2 methylenic units and of the corresponding polysiloxanes containing 11, 8, 6, and 3 methylenic units as flexible spacers were reported in a previous paper.[4]

0024-9297/89/2222-2062$01.50/0

Scheme I
Synthesis of 4-Hydroxy-4′-methoxy-α-methylstilbene

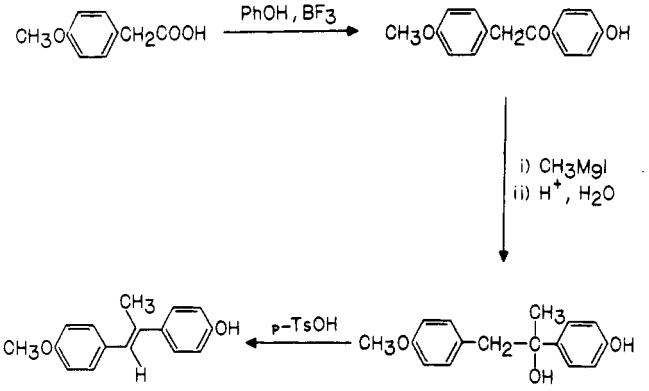

The goal of this paper is to describe the synthesis and characterization of polymethacrylates and polyacrylates containing mesogenic groups based on 4-hydroxy-4′-methoxy-α-methylstilbene and flexible spacers containing 11, 8, 6, 3, and 2 methylenic units and of the corresponding polysiloxanes containing 11, 8, 6, and 3 methylenic units as flexible spacers.

Experimental Section

Materials. Poly(methylhydrosiloxane) with number-average degree of polymerization 100 was synthesized in our laboratory. Its detailed synthesis is presented elsewhere.[14] Methacryloyl chloride and acryloyl chloride (both from Fluka), allyl bromide, 1,5-dibromopentane, 1,6-dibromohexane, 8-bromo-1-octene, 11-undecen-1-ol (all from Aldrich), 2-chloroethanol, 3-chloro-1-propanol, 6-chloro-1-hexanol, 8-chloro-1-octanol, 4-methoxyphenylacetic acid, phenol (all from Lancaster Synthesis), 11-bromo-1-undecanol (from Fluka), and BF_3 gas (Aldrich) were used as received. Toluene used in the hydrosilation reaction was first refluxed over sodium and then distilled under argon. 2,2′-Azoisobutyronitrile (AIBN, from Fluka) was freshly recrystallized from methanol (below 40 °C). Polymerization solvents were first refluxed under sodium and then distilled under argon. All the other reagents were used as received, unless otherwise specified.

Techniques. ^1H NMR (200-MHz) spectra were recorded on a Varian XL-200 spectrometer. All spectra were recorded in $CDCl_3$ solution with TMS as internal standard, unless noted. A Perkin-Elmer DSC-4 differential scanning calorimeter, equipped with a TADS 3600 data station, was used to determine the thermal transitions which were read at the maximum of their endothermic or exothermic peaks. In all cases, heating and cooling rates were 20 °C/min, unless otherwise specified. Glass transition temperatures (T_g) were read at the middle of the change in the heat capacity. All transitions were collected from second or further cooling scans, unless otherwise specified. A Carl-Zeiss optical polarized microscope (magnification: 100×) equipped with a Mettler FP 82 hot stage and a Mettler FP 800 central processor was used to observe the thermal transitions and to analyze the anisotropic textures.[15,16] Molecular weights were determined by gel permeation chromatography (GPC) with a Perkin-Elmer Series 10 LC instrument equipped with LC-100 column oven, LC-600 autosampler, and Sigma 15 data station. High-pressure liquid chromatography (HPLC) determinations were performed with the same instrument. The measurements were made by using an UV detector; THF as solvent (1 mL/min; 40 °C); a set of PL gel columns of 10^2, 5×10^2, 10^3, 10^4, and 10^5 Å; and a calibration plot constructed with polystyrene standards.

Synthesis of Monomers and Polymers. The synthesis of monomers and polymers is outlined in Schemes I–III.

4-Hydroxyphenyl 4-Methoxybenzyl Ketone. In a 500-mL three-neck flask equipped with thermometer, condenser, magnetic stirrer, and gas bubbler were added 4-methoxyphenylacetic acid (35.3 g, 0.2125 mol), phenol (20.0 g, 0.2125 mol), and 200 mL of CCl_4. The reaction mixture was heated to 60 °C under nitrogen atmosphere. BF_3 gas was bubbled slowly through the reaction mixture until saturation was reached (22.0 g, 0.3240 mol). Stirring

Scheme II
Synthesis of Polymethacrylates (4′-n-PMA) and Polyacrylates (4′-n-PAC) Containing 4-Hydroxy-4′-methoxy-α-methylstilbene Based Mesogens

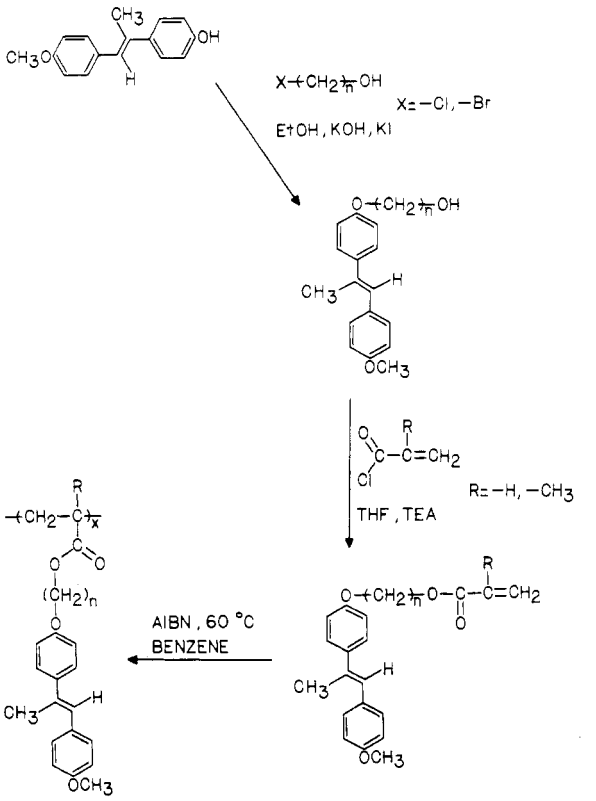

Scheme III
Synthesis of Polysiloxanes (4′-n-PS) Containing 4-Hydroxy-4′-methoxy-α-methylstilbene Based Mesogens

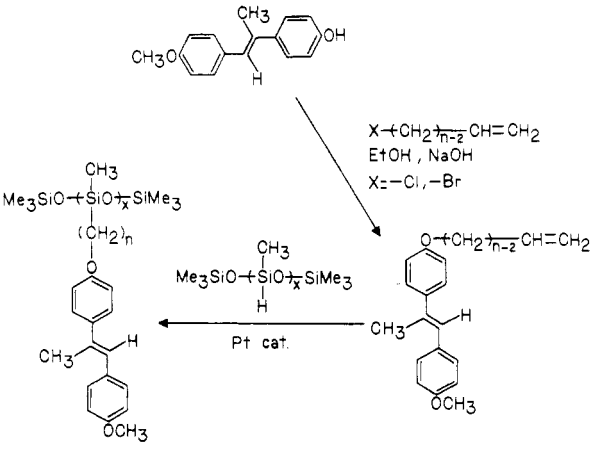

was continued for about 20 h at 60 °C. The reaction mixture was then cooled to room temperature, and the resulting viscous reaction mixture was treated with aqueous NaOH solution. The aqueous layer was separated and acidified with dilute HCl, and the resulting precipitate was filtered, washed with water, and dried. The crude product was recrystallized from methanol to yield 27.4 g (53%) of shiny crystals. Purity: 98% (HPLC). MP: 171–173 °C. ^1H NMR ($CDCl_3$ TMS, δ, ppm): 3.14 (OH, s), 3.77 (CH_3O, s), 4.21 (CH_2CO, s), 6.89 (2 aromatic protons ortho to hydroxy, d), 6.96 (2 aromatic protons ortho to methoxy, d), 7.24 (2 aromatic protons meta to methoxy, d), 8.00 (2 aromatic protons meta to hydroxy, d).

4-Hydroxy-4′-methoxy-α-methylstilbene (4′-MHMS). A 1-L three-neck flask equipped with nitrogen inlet–outlet, condenser, addition funnel, and magnetic stirrer and containing 7.23 g (0.2973 mol) of Mg turnings and a crystal of iodine was flame-dried and then cooled to room temperature. A solution of CH_3I (18.5 mL, 0.2973 mol) in 185 mL of dry diethyl ether was added dropwise

Table I
Characterization of 4-(ω-Hydroxyalkanyl-1-oxy)-4′-methoxy-α-methylstilbenes (4′-n-OH)

compd	yield, %	mp, °C	200-MHz ^{1}H NMR ($CDCl_3$, δ, ppm)
4′-11-OH	72	131	1.31–1.80 [m, —(CH_2)—$_9$], 2.26 (s, CH_3C=), 3.66 (t, CH_2O), 3.84 (s, CH_3O), 3.99 (t, CH_2OPh), 6.74 (s, PhC*H*=), 6.89–7.49 (m, 8 aromatic protons)
4′-8-OH	56	130	1.40–1.86 [m, —(CH_2)—$_6$], 2.24 (s, CH_3C=), 3.57 (t, CH_2O), 3.84 (s, CH_3O), 4.03 (t, CH_2OPh), 6.74 (s, PhC*H*=), 6.87–7.49 (m, 8 aromatic protons)
4′-6-OH	55	133	1.49–1.84 [m, —(CH_2)—$_4$], 2.23 (s, CH_3C=), 3.61 (t, CH_2O), 3.83 (s, CH_3O), 4.03 (t, CH_2OPh), 6.71 (s, PHC*H*=), 6.89–7.47 (m, 8 aromatic protons)
4′-3-OH	52	149	1.97 (t, CH_2), 2.26 (s, CH_3C=), 3.77 (t, CH_2O), 3.84 (s, CH_3O), 3.84 (s, CH_3O), 4.16 (t, CH_2OPh), 6.71 (s, PhC*H*=), 6.94–7.54 (m, 8 aromatic protons)
4′-2-OH	46	129	2.20 (s, CH_3C=), 3.80 (t, CH_2O), 3.86 (s, CH_3O), 4.10 (t, CH_2OPh), 6.76 (s, PhC*H*=), 6.94–7.51 (m, 8 aromatic protons)

Table II
Characterization of Methacrylates (4′-n-MA)

compd	yield, %	mp, °C	200-MHz ^{1}H NMR ($CDCl_3$, δ, ppm)
4′-11-MA	55	71	1.31–1.80 [m, —(CH_2)—$_9$], 1.96 (s, CH_3CCOO), 2.26 (s, CH_3C=), 3.84 (s, CH_3O), 3.99 (t, CH_2OPh), 4.16 (t, CH_2OOC), 5.56 and 6.13 (2s, CH_2=), 6.74 (s, PhC*H*=), 6.89–7.49 (m, 8 aromatic protons)
4′-8-MA	47	65	1.39–1.80 [m, —(CH_2)—$_6$], 1.94 (s, CH_3CCOO), 2.24 (s, CH_3C=), 3.86 (s, CH_3O), 4.00 (t, CH_2OPh), 4.17 (t, CH_2OOC), 5.57 and 6.11 (2s, CH_2=), 6.73 (s, PhC*H*=), 6.89–7.47 (m, 8 aromatic protons)
4′-6-MA	67	53	1.50–1.80 [m, —(CH)$_2$—$_4$], 1.94 (s, CH_3CCOO), 2.24 (s, CH_3C=), 3.83 (s, CH_3O), 4.00 (t, CH_2OPh), 4.19 (t, CH_2OOC), 5.57 and 6.13 (2s, CH_2=), 6.73 (s, PhC*H*=), 6.89–7.49 (m, 8 aromatic protons)
4′-3-MA	44	70	1.96 (s, CH_3CCOO), 1.17 (t, CH_2), 2.26 (s, CH_3C=), 3.83 (s, CH_3O), 4.10 (t, CH_2OPh), 4.37 (t, CH_2OOC), 5.57 and 6.16 (2s, CH_2=), 6.74 (s, PhC*H*=), 6.89–7.46 (m, 8 aromatic protons)
4′-2-MA	70	76	2.09 (s, CH_3CCOO), 2.26 (s, CH_3C=), 3.82 (s, CH_3O), 4.00 (t, CH_2OPh), 4.24 (t, CH_2OOC), 5.58 and 6.13 (2s, CH_2=), 6.71 (s, PhC*H*=), 6.89–7.47 (m, 8 aromatic protons)

Table III
Characterization of Acrylates (4′-n-AC)

compd	yield, %	mp, °C	200-MHz ^{1}H NMR ($CDCl_3$, δ, ppm)
4′-11-AC	48	86	1.31–1.76 [m, —(CH_2)—$_9$], 2.23 (s, CH_3C=), 3.83 (s, CH_3O), 3.97 (t, CH_2OPh), 4.17 (t, CH_2OOC), 5.77–6.46 (m, CH_2=C*H*), 6.73 (s, PhC*H*=), 6.89–7.46 (m, 8 aromatic protons)
4′-8-AC	61	88	1.39–1.78 [m, —(CH_2)—$_6$], 2.24 (s, CH_3C=), 3.82 (s, CH_3O), 3.97 (t, CH_2OPh), 4.16 (t, CH_2OOC), 5.78–6.43 (m, CH_2=C*H*), 6.70 (s, PhC*H*=), 6.86–7.43 (m, 8 aromatic protons)
4′-6-AC	51	85	1.51–1.83 [m, —(CH_2)—$_4$], 2.26 (s, CH_3C=), 3.84 (s, CH_3O), 4.00 (t, CH_2OPh), 4.20 (t, CH_2OOC), 5.81–6.47 (m, CH_2=C*H*), 6.74 (s, PhC*H*=), 6.90–7.49 (m, 8 aromatic protons)
4′-3-AC	43	87	2.17 (t, CH_2), 2.24 (s, CH_3C=), 3.84 (s, CH_3O), 4.10 (t, CH_2OPh), 4.39 (t, CH_2OOC), 5.83–6.49 (m, CH_2=C*H*), 6.73 (s, PhC*H*=), 6.90–7.49 (m, 8 aromatic protons)
4′-2-AC	45	105	2.26 (s, CH_3C=), 3.83 (s, CH_3O), 4.26 (t, CH_2OPh), 4.56 (t, CH_2OOC), 5.87–6.41 (m, CH_2=C*H*), 6.74 (s, PhC*H*=), 6.91–7.49 (m, 8 aromatic protons)

at such a rate as to maintain gentle reflux (about 1 h). After the addition was completed, the reaction mixture was stirred under reflux until all the Mg was dissolved. Then a solution of 24.0 g (0.0991 mol) of 4-hydroxyphenyl 4-methoxybenzyl ketone in 350 mL of dry tetrahydrofuran was added dropwise to keep the reaction mixture under reflux (2 h). After the addition was completed, the reaction mixture was stirred at room temperature overnight. Then it was cooled in an ice water bath and a saturated aqueous NH_4Cl solution was added dropwise under nitrogen until the white dispersion separated into organic and aqueous phases. The organic phase was separated, and the mixture of solvents was removed in a rotavapor. The remaining tertiary alcohol was dissolved in toluene, traces of *p*-toluenesulfonic acid were added, and the toluene was removed in a rotavapor. During this distillation process, the dehydration of the tertiary alcohol takes place, and the produced water is azeotropically distilled with toluene. The resulting solid was recrystallized from methanol to yield 17.1 g (72%) of white crystals. Purity: 99% (HPLC). MP: 149 °C (DSC, 20 °C/min). ^{1}H NMR [$(CD_3)_2CO$, TMS, δ, ppm]: 2.21 (CH_3C=, s), 3.09 (OH, s), 3.83 (CH_3O, s), 6.74 (PhCH=, s), 6.86 (2 aromatic protons ortho to hydroxy, d), 6.94 (2 aromatic protons ortho to methoxy, d), 7.31 (2 aromatic protons meta to hydroxy, d), 7.41 (2 aromatic protons meta to methoxy, d).

4′-Methoxy-4-(ω-hydroxyalkanyl-1-oxy)-α-methylstilbenes (4′-n-OH). All compounds were synthesized by the etherification of 4′-MHMS with the corresponding bromo or chloro alcohol in 70% ethanol and in the presence of KOH at reflux temperature. An example of this procedure is outlined below. KOH (0.911 g, 0.0162 mol) was dissolved in 100 mL of 70% ethanol. 4′-MHMS (3.90 g, 0.0162 mol) and 11-bromo-1-undecanol (4.49 g, 0.0179 mol) were added together with a small amount of KI to the reaction mixture, which was refluxed for 24 h. The alcohol was removed in a rotavapor and the resulting solid was washed successively with water, dilute aqueous NaOH, and water. Recrystallization from methanol yielded 4.77 g (72%) of white crystals. All compounds were repeatedly recrystallized until their purity was higher than 99% (HPLC). Yields, melting points, and protonic resonances are summarized in Table I.

Methacrylates and Acrylates of 4′-Methoxy-4-(ω-hydroxyalkanyl-1-oxy)-α-methylstilbenes (4′-n-MA, 4′-n-AC). All monomers were synthesized by the esterification of the corresponding alcohols (4′-n-OH) with methacryloyl or acryloyl chloride. An example is as follows. 4′-Methoxy-4-(hydroxyhexanyl-1-oxy)-α-methylstilbene (4′-6-OH; 1.50 g, 4.40 mmol) was dissolved in 100 mL of THF freshly distilled from $LiAlH_4$, and 0.77 mL (5.50 mmol) of dry triethylamine was added. The obtained solution was cooled to 0 °C in an ice water bath, and 0.51 mL (5.30 mmol) of methacryloyl chloride was added dropwise. The reaction mixture was allowed to warm to room temperature and was kept stirring overnight. The precipitated Et_3N·HCl was filtered, and the solvent was removed in a rotavapor at room temperature. The resulting solid was washed with an aqueous solution of $NaHCO_3$, water, filtered, dried, and recrystallized from methanol. To achieve purity higher than 99.0% (HPCL), all monomers required purification by column chromatography (silica gel, CH_2Cl_2 eluent). In the present case, after purification by column chromatography, we obtained 1.20 g (67%) of product. Yields, melting points, and protonic resonances are summarized in Tables II and III.

Radical Polymerization of Monomers. All monomers were polymerized in dry benzene using AIBN as initiator at 60 °C for 20 h. Polymerizations were carried out in Schlenk tubes under argon atmosphere after monomer solutions were degassed by several freeze–pump–thaw cycles under vacuum. The monomer and initiator concentrations for the polymerization of meth-

Table IV
Thermal Transition and Thermodynamic Parameters of Polymethacrylates (4′-n-PMA)

polymer	GPC $10^{-3}\bar{M}_n$	GPC $\bar{M}_w/\bar{M}_n$	phase transitions (°C) and corresponding enthalpy changes (kcal/mru) heating	cooling
4′-11-PMA	23.4	2.0	g 12 s 116 (1.25) i	i 105 (1.13) s 4 g
4′-11-PMA[a]	23.4	2.0	g 15 k 55 (0.55) k 83 (0.39) s 119 (0.99) i	i 105 (1.13) s 4 g
4′-8-PMA	24.1	2.0	g 18 s 55 (0.29) n 112 (0.43) i	i 108 (0.43) n 53 (0.21) s 15 g
4′-6-PMA	24.7	2.5	g 32 n 101 (0.26) i	i 97 (0.21) n 24 g
4′-3-PMA	43.6	2.5	g 55 s 85 (0.05) n 115 (0.17) i	i 110 (0.16) n 75 (0.03) s 42 g
4′-2-PMA	14.9	2.0	g 66 n 122[b] i	i 112[b] n 62 g

[a] Obtained from first heating and cooling scans. [b] Pseudohomeotropic, determined by optical polarized microscopy.

Table V
Thermal Transitions and Thermodynamic Parameters of Polyacrylates (4′-n-PAC)

polymer	GPC $10^{-3}\bar{M}_n$	GPC $\bar{M}_w/\bar{M}_n$	phase transition (°C) and corresponding enthalpy changes (kcal/mru) heating	cooling
4′-11-PAC	15.9	2.0	g 12 k 107 (2.86) s 115[a] (0.80) i	i 107 (0.72) s 37 (1.08) k 3 g
4′-8-PAC	12.2	1.8	g 11 s 66 (0.03) n 83 (0.39) k 99 (0.55) n 104 (0.07)[a]	i 97 (0.23) n 63 (0.03) s 6 g
4′-6-PAC	14.0	2.0	g 18 n 101 (0.11) i	i 97 (0.10) n 14 g
4′-6-PAC[b]	14.0	2.0	k 55 (1.09) n 103 (0.06) i	i 97 (0.10) n 14 g
4′-3-PAC	16.3	1.9	g 38 k 59 (0.02) n 81 (0.03) i	i 76 (0.10) n 14 g
4′-2-PAC	11.5	1.7	g 53 n 96[c] i	i 84[c] n 50 g

[a] Overlapped transitions. [b] First heating and cooling scans. [c] Pseudohomeotropic, determined by optical polarized microscopy.

Table VI
Characterization of 4-(ω-Alkenyl-1-oxy)-4′-methoxy-α-methylstilbene (4′-n-O)

compd	yield, %	mp, °C	200-MHz ^{1}H NMR ($CDCl_3$, δ, ppm)
4′-11-O	44	101	1.31–2.06 [m, $-(CH_2)-_8$], 2.26 (s, $CH_3C=$), 3.84 (s, CH_3O), 3.97 (t, CH_2O), 4.99 and 5.86 (m, $CH_2=CH$), 6.74 (s, PhC*H*=), 6.87–7.47 (m, 8 aromatic protons)
4′-8-O	70	96	1.41–2.10 [m, $-(CH_2)-_5$], 2.24 (s, $CH_3C=$), 3.83 (s, CH_3O), 3.97 (t, CH_2O), 4.96 and 5.83 (m, $CH_2=CH$), 6.71 (s, PhC*H*=), 6.86–7.46 (m, 8 aromatic protons)
4′-6-O	67	99	1.59–2.17 [m, $-(CH_2)-_3$], 2.26 (s, $CH_3C=$), 3.84 (s, CH_3O), 4.00 (t, CH_2O), 5.03 and 5.84 (m, $CH_2=CH$), 6.74 (s, PhC*H*=), 6.91–7.47 (m, 8 aromatic protons)
4′-3-O	73	111	2.24 (s, $CH_3C=$), 3.84 (s, CH_3O), 4.59 (t, CH_2O), 5.37 and 6.06 (m, $CH_2=CH$), 6.73 (s, PhC*H*=), 6.90–7.47 (m, 8 aromatic protons)

Table VII
Thermal Transitions and Thermodynamic Parameters of Polysiloxanes (4′-n-PS)

polymer	GPC $10^{-3}\bar{M}_n$	GPC $\bar{M}_w/\bar{M}_n$	phase transitions (°C) and corresponding enthalpy changes (kcal/mru) heating	cooling
4′-11-PS	13.4	1.8	k 127 (3.81) s 138 (1.20)[a] i	i 131 (0.76) s 90 (3.75) k
4′-8-PS	16.4	2.0	k 128 (4.46) i	i 117 (0.22) n 89 (3.54) k
4′-6-PS	19.6	1.8	g 10 k 124 (3.95) i	i 103 (0.09) n 81 (3.09) k
4′-3-PS	14.3	2.0	g 22 k 84 (1.43) n 110 (0.12) i	i 107 (0.10) n 65 (1.33) k

[a] Overlapped transition.

acrylates were 20% (w/v) and 0.5% (w/w) monomer, respectively, while those for the polymerization of acrylates were 20% (w/v) and 0.25% (w/w) monomer, respectively. After polymerization, the reaction mixture was diluted with benzene and precipitated into methanol. The filtered polymers were dried under vacuum and then were purified by successive reprecipitations from THF solution into acetone and methanol until GPC curves showed no traces of unreacted monomer or oligomers. The characterization of the resulting polymers is presented in Tables IV and V.

5-Bromo-1-pentene and 6-Bromo-1-hexene. Both compounds were synthesized according to a literature procedure.[7] Their detailed synthesis was previously described.[3]

11-Chloro-1-undecene. It was prepared as previously described.[3]

4-(ω-Alkenyl-1-oxy)-4′-methoxy-α-methylstilbenes (4′-n-O). All compounds were synthesized by the etherification of 4′-MHMS with the corresponding bromo- or chloroalkene. An example is outlined below. Freshly cut sodium (0.192 g, 8.33 mmol) was dissolved in 60 mL of absolute ethanol. To the resulting solution were added 2.0 g (8.33 mmol) of 4′-MHMS and 0.701 g (9.16 mmol) of allyl chloride. The reaction mixture was refluxed for 24 h. Ethanol was removed in a rotavapor, and the resulting solid was washed with water, dilute NaOH aqueous solution, and water, filtered and recrystallized from methanol. The white product was further purified (purity higher than 99% HPLC) by column chromatography (silica gel, CH_2Cl_2 eluent) to yield 1.71 g (73%). The ^{1}H NMR chemical shifts of all derivatives together with their melting temperatures and conversions are presented in Table VI. The purity of these compounds was higher than 99% in all cases.

Synthesis of Polysiloxanes (4-n-PS). The synthesis of polysiloxanes is outlined in Scheme III. A general procedure is described below. The olefinic derivative (4′-n-O); 1.0 g, 10 mol % excess versus Si–H groups present in polysiloxane) was dissolved in 100 mL of dry, freshly distilled toluene together with the proper amount of poly(methylhydrosiloxane). The reaction mixture was heated to 110 °C under nitrogen, and 100 μg of dicyclopentadienylplatinum(II) chloride catalyst[18] was then injected with a syringe as solution in methylene chloride (1 mg/mL). The reaction mixture was refluxed (110 °C) under nitrogen until both IR and 200-MHz ^{1}H NMR analyses showed that all the Si–H groups were consumed (about 24–30 h). The white polymers were separated by precipitation into methanol and were purified by successive precipitations from chloroform solutions into acetone and methanol until GPC traces showed the polymers to be free of unreacted 4′-n-O derivative. In order to avoid the contamination of the resulting polymers with polydimethylsiloxane from silicone grease or silicon oil, only Teflon tape and Teflon gaskets were used in the hydrosilation equipment. Table VII summarizes

the characterization of liquid crystalline polysiloxanes.

Results and Discussion

4-Hydroxy-4′-methoxy-α-methylstilbene was synthesized according to the reaction route outlined in Scheme I. The acylation of phenol with 4-methoxyphenylacetic acid was performed in thee presence of BF_3 gas as catalyst. As expected,[19,20] the use of BF_3 provides the acylation of phenol only in its para position and at the same time avoids the cleavage of the methoxy group of the 4-methoxyphenylacetic acid. The addition of CH_3MgI to 4-hydroxyphenyl 4-methoxybenzyl ketone and the dehydration of the resulting alcohol proceeded with high yields and did not provide any side reactions.

Tables IV, V, and VII summarize the molecular weights and the thermal transitions of all polymers. Although molecular weights are only relative, since they were obtained by using a calibration plot constructed with polystyrene standards, they can be used to estimate whether they are below or above the molecular weight whose phase transitions are molecular weight dependent. Recent results from our laboratory concerning the influence of molecular weight on the phase transitions of some of these polymethacrylates have demonstrated that, above number-average molecular weights of about 10 000, polymer phase transitions are not any more dependent (or are only very little dependent) on their molecular weight.[14,21,22] Therefore, as Tables IV, V, and VII show, all polymers have higher molecular weights than the value below which their phase transitions are molecular weight dependent.

Consequently, we can discuss, at least in a semiquantitative manner, the influence of the three different polymer backbones on the phase transitions and thermodynamic parameters of the corresponding polymers containing identical numbers of methylenic units in their flexible spacer.

Figure 1 presents some representative normalized DSC traces of the polymers containing 11 methylenic units in their flexible spacer. All three polymers exhibit an enantiotropic S_A mesophase, which displays on the optical polarized microscope a fan-shaped focal conic texture. There is no large difference between the isotropization temperatures of 4′-11-PMA and 4′-11-PAC. However, the isotropization transition of the 4′-11-PS appears at a temperature which is over 20 °C higher than that of the corresponding polymethacrylate and polyacrylate. When making this statement, we have to be aware of the fact that the flexible spacer of polysiloxane contains only 11 methylenic units, while the same flexible spacer in a polymethacrylate and polyacrylate contains 11 methylenic units plus an oxygen and a carbonyl group. Therefore, the flexible spacer of the polysiloxane is in fact shorter than the one of the polymethacrylate or polyacrylate. A quick inspection of the data in Table IV shows that in the case of polymethacrylates with long polymethylenic spacers there is no significant dependence of the isotropization temperature on the number of methylenic units in the spacer. However, the isotropization temperature shows a small increase in the case of polyacrylates (Table V) and a larger increase in the case of polysiloxanes (Table VII) containing long flexible spacers. On the basis of this discussion, we can conclude that the higher isotropization temperature exhibited by 4′-11-PS versus 4′-11-PAC and 4′-11-PMA is most probably the result of the different polymer backbone. An additional interesting remark refers to the fact that, while the isotropization enthalpies of 4′-11-PS (Table VII) and 4′-11-PAC (Table V) are almost equal, the isotropization enthalpy of 4′-11-PMA is larger (Table VI). All these enthalpies refer to data collected

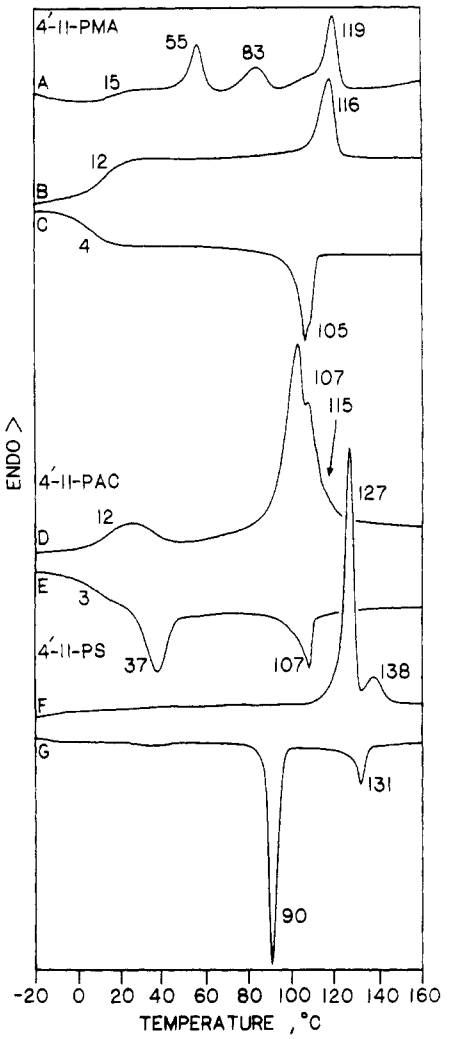

Figure 1. Normalized DSC traces of (A) 4′-11-PMA, first heating scan; (B) 4′-11-PMA, second and subsequent heating scans; (C) 4′-11-PMA, second and subsequent cooling scans; (D) 4′-11-PAC, second and subsequent heating scans; (E) 4′-11-PAC, second and subsequent cooling scans; (F) 4′-11-PS, second and subsequent heating scans; and (G) 4′-11-PS, second and subsequent cooling scans.

from the cooling scans. They are more reliable than the results obtained from the heating scans where isotropization and melting transitions are overlapped (Figure 1).

An additional major difference resulting from the use of different polymer backbones consists in the ability of the polymer to undergo side-chain crystallization. As we can observe from Figure 1, 4′-11-PMA exhibits melting transitions only during the first heating scan (curve A). Second and subsequent heating (curve B) and cooling (curve C) scans do not show melting or crystallization transitions. However, long-time annealing above the glass transition temperature of the polymethacrylate reinduces side-chain crystallization of this polymer. By increasing the flexibility of the polymer backbone from polymethacrylate to polyacrylate and subsequently to polysiloxane, we observe an enhanced ease of side-chain crystallization, as well as an increase of both melting and crystallization transition temperatures (Figure 1). An additional important observation consists in the decreased degree of supercooling of the crystallization transition temperature by increasing the flexibility of the polymer backbone (curves D–G from Figure 1). While in the case of polysiloxane this supercooling represents only 37 °C, in the case of polyacrylate it is as large as 100 °C. Therefore, even at this early stage of our discussion, we have to realize that

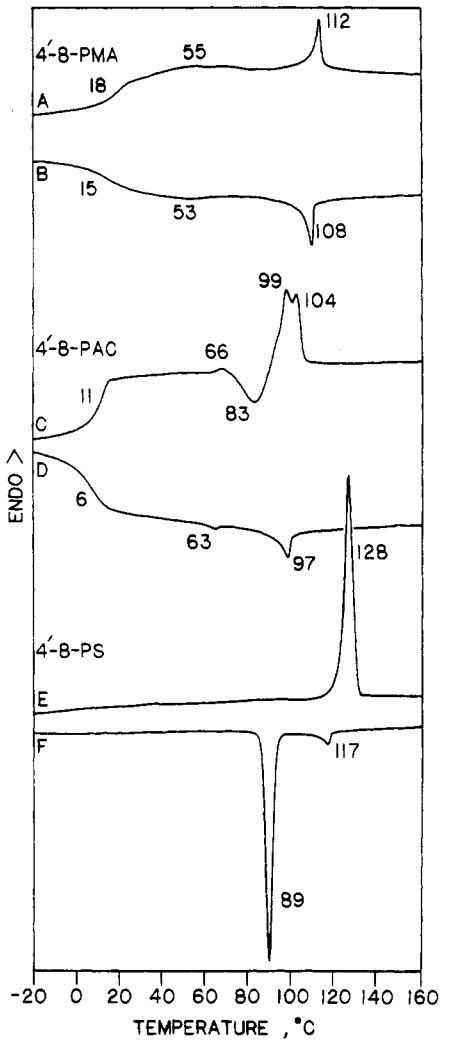

Figure 2. Normalized DSC traces of (A) 4'-8-PMA, second and subsequent heating scans; (B) 4'-8-PMA, second and subsequent cooling scans: (C) 4'-8-PAC, second and subsequent heating scans; (D) 4'-8-PAC, second and subsequent cooling scans; (E) 4'-8-PS, second and subsequent heating scans; and (F) 4'-8-PS, second and subsequent cooling scans.

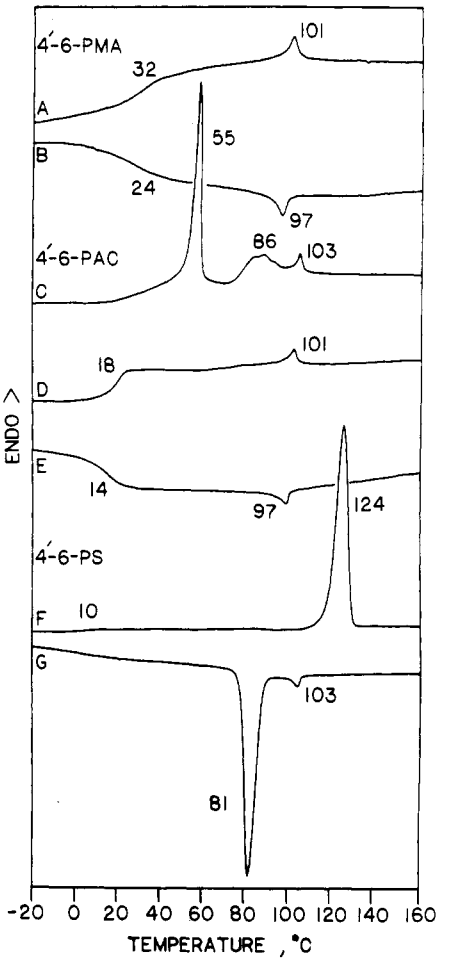

Figure 3. Normalized DSC traces of (A) 4'-6-PMA, second and subsequent heating scans; (B) 4'-6-PMA, second and subsequent cooling scans; (C) 4'-6-PAC, first heating scan; (D) 4'-6-PAC, second and subsequent heating scans; (E) 4'-6-PAC, second and subsequent cooling scans; (F) 4'-6-PS, second and subsequent heating scans; and (G) 4'-6-PS, second and subsequent cooling scans.

for a similar spacer length the role of the polymer backbone in affecting the nature and the kinetics of phase transitions is very important.

Let us now inspect very briefly the behavior of the polymers containing eight methylenic units in their flexible spacer (Figure 2). Both 4'-8-PMA (Figure 2, curves A, B; and Table IV) and 4'-8-PAC (Figure 2, curves C, D; and Table V) exhibit an enantiotropic nematic mesophase which presents a characteristic schlieren nematic texture on the optical polarized microscope and an unassigned enantiotropic smectic mesophase. However, 4'-8-PS exhibits only a monotropic nematic mesophase (Figure 2, curves E, F; and Table VII). As in the previous set of polymers, the highest isotropization temperature is exhibited by the polymer containing a polysiloxane backbone. Also as in the previous set of polymers, the highest enthalpy of isotropization is displayed by 4'-8-PMA (Table IV). 4'-8-PAC (Table V) and 4'-8-PS (Table VII) present almost equal but at the same time lower isotropization enthalpies than the corresponding polymethacrylate (Table VII). The difference between the monotropic versus the enantiotropic character of the mesophases exhibited by these polymers seems to be the result of their different tendency toward side-chain crystallization. The polymethacrylate does not undergo side-chain crystallization and therefore can reveal both nematic and smectic enantiotropic mesophases (Figure 2, curves A, B). However, both 4'-8-PAC (Figure 2, curves C, D) and 4'-8-PS (Figure 2, curves E, F) undergo side-chain crystallization. The crystallization transition of 4'-8-PAC is so much supercooled that it does not appear at all on the cooling scan of the DSC trace (Figure 2, curve D), but only on the heating scan (Figure 2, curve C). Since on the heating scan crystallization takes place right above the transition from smectic to nematic (Figure 2, curve C), we can consider that this smectic mesophase is enantiotropic. However, due to the proximity of the smectic–nematic and crystallization transitions, these two transitions are difficult to separate on the optical polarized microscope. On going to a more flexible backbone, like polysiloxane, the ease of side-chain crystallization increases. As a consequence, the melting transition overlaps the nematic–isotropic transition and the nematic mesophase becomes monotropic (Figure 2, curves E, F). At the same time, since crystallization is only slightly supercooled, it does not allow the smectic mesophase to be revealed even as a monotropic mesophase.

A similar trend can be observed in the behavior of the polymers containing six methylene units in their flexible spacer (Figure 3). 4'-6-PMA (Figure 3, curves C–E) exhibits enantiotropic nematic mesophases, while 4'-6-PS displays only a monotropic nematic mesophase (Figure 3, curves F, G). The highest isotropization temperature is exhibited by the polymer containing a polysiloxane backbone. Again the isotropization enthalpies of polysiloxane

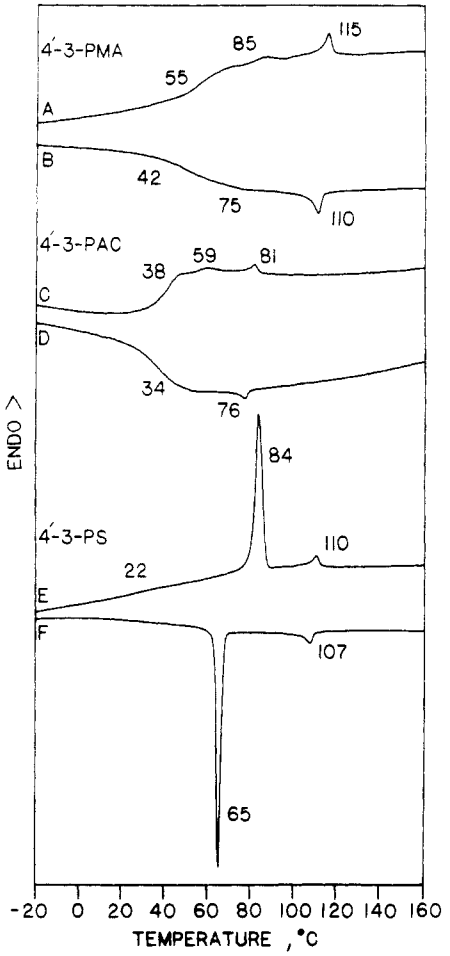

Figure 4. Normalized DSC traces of (A) 4'-3-PMA, second and subsequent heating scans; (B) 4'-3-PMA, second and subsequent cooling scans; (C) 4'-3-PAC, second and subsequent heating scans; (D) 4'-3-PAC, second and subsequent cooling scans; (E) 4'-3-PS, second and subsequent heating scans; and (F) 4'-3-PS, second and subsequent cooling scans.

(Table VII) and polyacrylate (Table V) are both equal and lower than that of the corresponding polymethacrylate (Table IV). As in the two situations discussed previously, the enantiotropic versus monotropic nature of the mesophase is primarily dictated by the ability of the polymer to undergo side-chain crystallization. While 4'-6-PMA does not undergo side-chain crystallization, 4'-6-PAC displays the melting of the crystallized side chains only during the first heating scan. However, in this case the melting temperature is below the isotropization transition temperature. Nevertheless, in the case of polysiloxane the melting transition temperature increases and overlaps the isotropization transition temperature. This event transforms the nematic mesophase from enantiotropic into monotropic.

Representative DSC traces of the polymers containing three methylenic units within their flexible spacer are presented in Figure 4. 4'-3-PMA exhibits nematic and smectic enantiotropic mesophases (Figure 4, curves A, B). Both 4'-3-PAC (Figure 4, curves C, D) and 4'-3-PS (Figure 4, curves E, F) exhibit enantiotropic nematic mesophases and side-chain crystallization. The relationship between the nature of the polymer backbone and the isotropization transition temperature is not as clear as in the previous examples. Only the side-chain crystallization tendency follows the same trend. It is somehow unique that the polymethacrylate exhibits the highest isotropization transition temperature (Figure 4) from all polymers. This could very well be the result of the much higher molecular weight of the polymethacrylate (Table IV) compared to that of the polyacrylate (Table V) and polysiloxane (Table VII). It is well established that, for the case of side-chain liquid crystalline polymers, the isotropization transition temperature increases very sharply with the increase of polymer molecular weight within the range of low molecular weights (typically up to number-average molecular weights of 10000–12000) and then increases only very little.[7,14,21,22] However, the corresponding isotropization enthalpy is molecular weight independent.[21,23] The trend observed for the isotropization enthalpies of these polymers obeys the same trend as that of the other series of polymers. That is, the enthalpy of isotropization of 4'-3-PMA (Table IV) is higher than that of 4'-3-PAC (Table V) and of 4'-3-PS (Table VII). The isotropization enthalpies of the last two polymers are within experimental error equal.

Although only for two different backbones, the trend followed by the isotropization temperature observed for the polymers containing three methylenic units in their flexible spacer seems to be similar to that of the polymers containing two methylenic units in their flexible spacer (Table IV and V). Both 4'-2-PMA and 4'-2-PAC display pseudohomeotropic nematic mesophases. The isotropization transition temperature of the polymethacrylate is higher than that of the corresponding polyacrylate (Tables IV and V).

Finally we could make some comments on the influence of spacer length on the type and nature of phase transitions within each series of polymers based on the same polymer backbone.

All polymethacrylates (Table IV) exhibit enantiotropic liquid crystalline mesophases. The isotropization transition temperature decreases with the decrease of the spacer length from 11 methylenic units to 6 and then increases again. The isotropization enthalpy increases with the increase in the spacer length. The polymethacrylate containing only two methylenic units in the flexible spacer displays only a nematic mesophase. Polymers containing intermediary spacer length display both smectic and nematic mesophases, while the polymethacrylate containing 11 methylenic units in the spacer displays only a smectic mesophase. Only the polymethacrylate containing 11 methylenic units in the flexible spacer exhibits side-chain crystallization. This side-chain crystallization is strongly kinetically controlled and can be best observed during the first heating scan.

Polyacrylates (Table V) behave similar to polymethacrylates with the exception that all undergo side-chain crystallization. For long spacers, this crystallization is observable on any DSC scan. However, for shorter spacers it can be observed mostly on the first heating scan or upon annealing.

All polysiloxanes (Table VII) undergo side-chain crystallization, and their isotropization transition temperatures are higher than those of the corresponding polymethacrylates or polyacrylates. The type of mesophase displayed by polysiloxane is determined, as in the case of other backbones, only by the spacer's length. However, the ease of side-chain crystallization can transform the highest temperature mesomorphic phase from enantiotropic into monotropic. This is the case of the polysiloxanes containing eight and six methylenic units within their flexible spacer.

The most general conclusion derived from these experiments is that the spacer length dictates the nature of the mesophase exhibited by a certain polymer. However, the nature of the polymer backbone dictates the thermal stability of the mesophase and the ease of side-chain

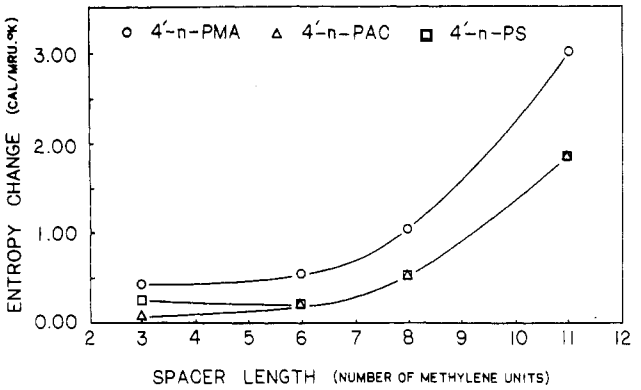

Figure 5. Dependence between the entropy change, ΔS (in cal/(mru K)), and the number of methylenic units in the flexible spacer (n) of (O) polymethacrylates (4'-n-PMA), (Δ) polyacrylates (4'-n-PAC), and (□) polysiloxanes (4'-n-PS).

crystallization. Flexible backbones tend to give rise to higher thermal stability of the mesophase and simultaneously to increased ease of side-chain crystallization. This last effect may lead to the transformation of enantiotropic mesophases into monotropic mesophases. All these results agree with previous data on the influence of polymer backbone on phase transitions in side-chain liquid crystalline polymers,[3,4,7,23] and the observed trend is not unexpected. These experiments have also provided a result which cannot be explained in a trivial way. It refers to the influence of polymer backbone on the isotropization transition temperatures and the enthalpy or entropy changes associated with these transitions. Figure 5 presents the plot of isotropization entropy as a function of spacer length for polymethacrylates, polyacrylates, and polysiloxanes. As mentioned previously, the trend is clear. The entropy change associated with the isotropization transition for polymethacrylates is higher than that of polyacrylates and polysiloxanes although their isotropization temperatures are reversed. The safest conclusion is that at the present time we have no explanation for this behavior.

Acknowledgment. We are grateful to the Office of Naval Research for the financial support of this work.

Registry No. 4'-MHMS, 109888-74-6; 4'-11-OH, 109888-78-0; 4'-8-OH, 118418-12-5; 4'-6-OH, 109888-76-8; 4'-3-OH, 118418-13-6; 4'-2-OH, 118418-14-7; 4'-11-MA, 109835-57-6; 4'-8-MA, 118400-11-6; 4'-6-MA, 109835-54-3; 4'-3-MA, 118400-14-9; 4'-2-MA, 118400-16-1; 4'-11-AC, 118400-18-3; 4'-8-AC, 118400-20-7; 4'-6-AC, 118400-22-9; 4'-3-AC, 118400-24-1; 4'-2-AC, 118400-26-3; 4'-11-PMA, 118400-10-5; 4'-8-PMA, 118400-12-7; 4'-6-PMA, 118400-13-8; 4'-3-PMA, 118400-15-0; 4'-2-PMA, 118400-17-2; 4'-11-PAC, 118400-19-4; 4'-8-PAC, 118400-21-8; 4'-6-PAC, 118400-23-0; 4'-3-PAC, 118400-25-2; 4'-2-PAC, 118400-27-4; 4'-11-O, 118400-28-5; 4'-8-O, 118400-30-9; 4'-6-O, 118400-32-1; 4'-3-O, 118400-34-3; 4-hydroxyphenyl 4'-methoxybenzyl ketone, 3669-46-3; 4-methoxyphenylacetic acid, 104-01-8; phenol, 108-95-2; 11-bromo-1-undecanol, 1611-56-9; methacryloyl chloride, 920-46-7; allyl chloride, 107-05-1.

References and Notes

(1) Percec, V.; Rodriguez-Parada, J. M.; Ericsson, C.; Nava, H. *Polym. Bull.* **1987**, *17*, 353.
(2) Percec, V.; Tomazos, D. *Polym. Bull.* **1987**, *18*, 239.
(3) Percec, V.; Hsu, C. S.; Tomazos, D. *J. Polym. Sci., Part A: Polym. Chem.* **1988**, *26*, 2047.
(4) Percec, V.; Tomazos, D. *J. Polym. Sci., Part A: Polym. Chem.*, in press.
(5) Hahn, B.; Percec, V. *Macromolecules* **1987**, *20*, 2961.
(6) Percec, V. *Mol. Cryst. Liq. Cryst.* **1988**, *155*, 487.
(7) Percec, V.; Pugh, C. In *Side Chain Liquid Crystalline Polymers*; McArdle, C. B., Ed.; Blackie and Sons, Ltd.: Glasgow, 1988, in press.
(8) Geib, H.; Hisgen, B.; Pschorn, U.; Ringsdorf, H.; Spiess, H. W. *J. Am. Chem. Soc.* **1982**, *104*, 917.
(9) Spiess, H. W. *Pure Appl. Chem.* **1985**, *57*, 1617.
(10) Boeffel, C.; Spiess, H. W.; Hisgen, B.; Ringsdorf, H.; Ohm, H.; Kirste, R. G. *Makromol. Chem., Rapid Commun.* **1986**, *7*, 777.
(11) Boeffel, C.; Hisgen, B.; Pschorn, U.; Ringsdorf, H.; Spiess, H. W. *Isr. J. Chem.* **1983**, *23*, 388.
(12) Engel, M.; Hisgen, B.; Keller, R.; Kreuder, W.; Reck, B.; Ringsdorf, H.; Schmidt, H. W.; Tschirner, P. *Pure Appl. Chem.* **1985**, *57*, 1009.
(13) Wassmer, K. H.; Ohmes, E.; Portugall, M.; Ringsdorf, H.; Kothe, G. *J. Am. Chem. Soc.* **1985**, *107*, 1511.
(14) Percec, V.; Hahn, B. *Macromolecules*, in press.
(15) Demus, D.; Richter, L. *Textures of Liquid Crystals*; Verlag Chemie: Weinheim, 1978.
(16) Gray, G. W.; Goodby, J. W. *Smectic Liquid Crystals. Textures and Structures*; Leonard Hill: Glasgow, 1984.
(17) Kraus, G. A.; Landgrebe, K. *Synthesis* **1984**, *17*, 885.
(18) Hsu, C. S.; Rodriguez-Parada, J. M.; Percec, V. *J. Polym. Sci., Part A: Polym. Chem.* **1987**, *25*, 2425.
(19) Buu-Hoi, N. P.; Seailles, J. *J. Org. Chem.* **1955**, *20*, 606.
(20) Armstrong, E. C.; Bent, R. L.; Loria, A.; Thirtle, J. R.; Weissberger, A. *J. Am. Chem. Soc.* **1960**, *82*, 1928.
(21) Percec, V.; Tomazos, D.; Pugh, C. *Macromolecules*, in press.
(22) Stevens, H.; Rehage, G.; Finkelmann, H. *Macromolecules* **1984**, *17*, 851.
(23) Percec, V.; Hahn, B. *J. Polym. Sci., Part A: Polym. Chem.*, in press.